Chapter 1.2

STUDIES ON SUBCRITICAL CRACK GROWTH IN FAÇADE ROCK PANEL USING FOUR-POINT BENDING

K.W. Kwok[1], R.H.C. Wong[1], K.T. Chau[1] and T.-f. Wong[2]
[1]*Dept. of Civil and Structural Engng, The Hong Kong Polytechnic University, H.K., China;*
[2]*Depts. of Geosciences and Mech. Engng, State University of New York at Stony Brook, USA*

Abstract: Thin rock panels are commonly used on exterior cladding walls in high-rise buildings. However, it has been found that these rock panels on exterior cladding may develop long-term time-dependent cracking, due to stress concentrations induced by periodic wind load and sunshine, and stress corrosion due to environmental effects (such as acid rain). This kind of cracking at stress level lower than that required for overcoming fracture toughness can be explained by using the concept of subcritical crack growth (SCG) of the pre-existing microcracks. However, existing design requirements of rock panel do not account for SCG. The standard testing method for SCG is the double torsion test (DTT), which does not simulate the failure condition of rock panel under wind and sunshine. Thus, a new method is introduced to investigate the SCG in rock panel under different environmental conditions: the four-point bending (4PB) test. Rock panel specimens containing a central notch were immersed in water, acid and air buffer during the loading test. For comparison DTTs were also conducted. It was found that the crack growth rate increases drastically if the cracked specimen is moved from a water buffer to a set-up with an acidic buffer. The SCG index n (a larger value indicates a faster crack growth) obtained by 4PB test is found consistently lower than that determined by DTT. This may be due to the different fracture mechanisms activated. One distinct feature of the 4PB test is that the SCG in rock panel is monitored through the crack length measurement whereas no such measurement is possible in DTT.

Key words: façade rock panel; subcritical crack growth; four-point bending test; granite; double torsion test.

1. INTRODUCTION

Traditionally, rock panels have been used for façade cladding for their aesthetic appearance. However, rock panels on exterior cladding walls are subjected to mechanical loads due to wind pressure, thermal loads due to sun-

S.K. Kourkoulis (ed.), Fracture and Failure of Natural Building Stones, 19–34.

Figure 1. Typical cracking on granite cladding panels (Chew et al.[1]).

shine, and chemical corrosions due to polluted moisture air. Due to these loading and corrosion, cracking is not uncommon on rock panels in exterior cladding after several years of exposure to these external effects and loads. This is particular so for the case of thin rock slabs (< 30mm). Figure 1 shows some examples of cracking of rock panels on building façade.

Although rock panels have been widely used on exterior cladding walls and cracking in rock panels has been reported repeatedly worldwide, there is still no internationally accepted design standard for rock panels or slabs[2]. There are, however, various design codes in different countries for testing the mechanical properties of dimensional stones for cladding installation, but none of these codes requires testing the fracture properties of rock. In the conclusion of Bayer and Clift[3], they mentioned that the use of Fracture Mechanics might be important for designing rock cladding wall. Motivated by this application, Chau and Shao[4] developed the first Fracture Mechanics based model in predicting the life of rock panels subjected to periodic sunshine using the concept of subcritical crack growth.

According to the classical theory of linear Fracture Mechanics, a crack is considered to be stable and does not grow when the stress intensity factor K_I at a crack tip is smaller than the critical stress intensity factor K_{IC} or the fracture toughness. However, as summarized by Atkinson[5] a crack can propagate even at a value of K_I smaller than that of the critical value (i.e. fracture toughness, K_{IC}). In geophysics, such crack growth phenomenon is referred as subcritical crack growth (SCG). Crack growth in rock panel appears only years after its completion and crack propagation appears to occur under service loadings. This indicates that crack growth in rock panels induced by periodic thermal loading due to sunshine and corrosion may be considered as a kind of SCG. This is the idea behind the model proposed by Chau and Shao[4]. However, the existing SCG parameters have been obtained mainly under the double torsion test which is quite different from the cracking mode in external cladding. Therefore, it is worthwhile to investigate the fracture behavior of rock panels under bending, which is believed to be the main loading mode on rock panels.

The time for rock panel to crack substantially depends on the rate of SCG, *da/dt* where *da* is the crack growth length and *dt* is the corresponding time interval. The relation between the SCG rate and the K_I can be determined by the power law suggested by Charles[6] and modified by Miura et al.[7] and others:

$$da/dt = v_0 (K_I/K_0)^n \quad (1)$$

where v_0 and n the crack velocity at $K_I=K_0$ and the SCG index respectively. These two important parameters depend on the type of rock and on environmental effects such as acidity and temperature of the atmosphere. Previous experimental data[8] suggested that there are three regions of SCG for most homogenous materials like ceramics and glass (Figure 2). The main factor affecting the crack growth was explained by the chemical reaction near the crack tip at low K_I (region I), the diffusion of corrosive species to the crack tip at intermediate K_I (region II) and mechanical rupture at large K_I (region III).

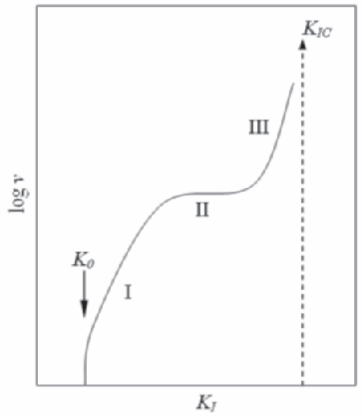

Figure 2. Schematic stress intensity factor/crack velocity diagram (Evans[8]).

Atkinson[5] summarized a wide range of SCG studies on granitic rocks using DTT method and the majority of the results indicated a linear log K_I – log v graph, which is different from that with three regions shown in Figure 2. This crack growth behavior is investigated in the present study.

Although double torsion test has been adopted by many researchers[5, 8-14], for testing the subcritical cracking parameters, as remarked earlier rock panels

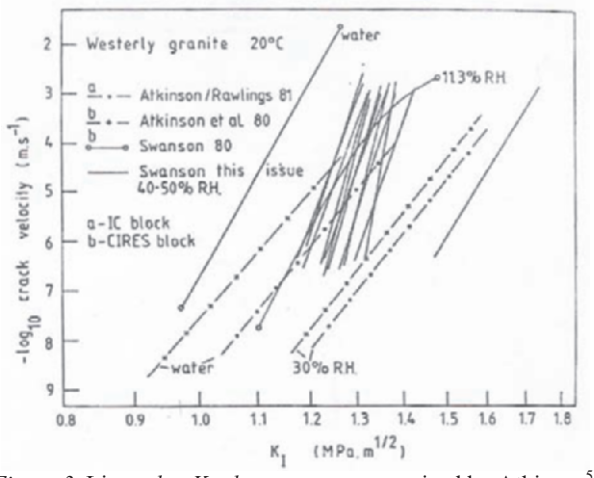

Figure 3. Linear *log K – log v* curve summarized by Atkinson[5].

are likely to bend under both thermal stress induced by sunshine and wind loads. Thus, to simulate a more realistic condition of cracking, 4PB test is proposed for subcritical cracking test in this study. It should be noted that the bending stress is constant in the middle one-third of the rock panel under four-point bending test. For comparison reasons, DTTs were also carried out. Both the $K - v$ curve and the SCG index n are compared.

2. EXPERIMENTAL DETAILS

In this section, the 4PB test method is first presented. Both the theory and the experimental setup are described in details in the following sections.

2.1 Four-point bending test method

2.1.1 Specimen preparation

The rock samples used in this study are fine-grained granite purchased from Fujian, China. The rock contains about 50-55% feldspar, 30-35% quartz, 8-10% mica, and 1-2% opaque minerals. The physical properties of the rock specimen are: density, ρ=2630 kg/m^3; compressive strength, σ_c=197 MPa; indirect tensile strength, σ_t=9.6 MPa; Young's modulus, E=54 GPa; Poisson's ratio, υ=0.387; and porosity=0.9%. The dimensions of the specimens are 300 mm × 30mm × 20mm. Both top and bottom surfaces of all samples are grinded and polished to within a deviation of less than 0.05 mm from the target size using grinding machine. A notch is introduced by a cutting saw. The notch depth (a_0) to thickness (a/W) ratio is 0.5 and the notch width is approximately 1 mm (note that a/W ratio should not be greater than 0.7 according to Murakami[15]). Pre-cracking (a small natural crack is first created at the notch by a small loading) is a general practice used in the double torsion test in studying subcritical crack growth. However, as it was difficult to obtain a stable pre-crack in the 4PB test (it is an inherent unstable test), the specimen is not pre-cracked in this study.

2.1.2 Experimental setup

4PB tests are performed using a four-point bending fixture with inner and outer spans of 200mm and 240mm respectively (Figure 4). Both for the loading points and the supports steel rollers are used. The load P is induced as dead weight and it is recorded by a load cell. A clip gauge is used to record the crack mouth opening displacement. Then the growth of crack length, Δa can be determined by compliance calibration (which will be discussed in §2.1.4). The experimental setup of the 4PB test is shown in Figure 5.

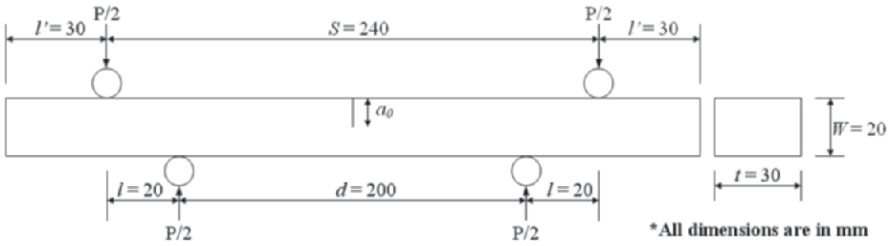

Figure 4. Schematic diagram of rock specimen subjected to 4PB test.

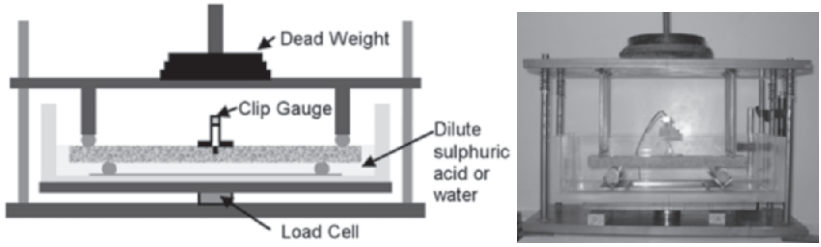

Figure 5. Experimental setup of 4PB test.

2.1.3 Determination of stress intensity factor (K_I)

The Stress Intensity Factor (SIF) K_I at the central notch tip can be calculated in terms of the applied load P by the following formula (Murakami[15]):

$$K_I = (3Pl/tW^2) \times (\pi a)^{1/2} \times F_{IM}(\alpha) \quad (2)$$

$$F_{IM}(\alpha) = 1.122 - 1.121\alpha + 3.74\alpha^2 + 3.873\alpha^3 - 19.05\alpha^4 + 22.55\alpha^5 \quad (3)$$

where $\alpha = a/W$ and a is the current crack length defined as the sum of the crack growth (Δa) and the notch length (a_0). The geometric parameters l and t are defined in Figure 4. The fracture toughness can be determined by substituting the critical loading P_c (when crack growth starts) in place of P in Eq.(2) and setting K_I to K_{IC}.

2.1.4 Crack length determination by using compliance calibration

The growth of crack length is monitored by the crack mouth opening displacement (CMOD). The CMOD is measured as a function of time by a clip gauge mounted at the two edges of the notch (Figure 5). The calibration between CMOD and crack length is conducted according to the calibration method proposed by Schmidt[16].

The specimen with a notch length a_1 is loaded with dead weight using the setup mentioned in §2.1.2. The CMOD is measured by a clip gauge and the corresponding load is measured by a load cell. The initial slope of the load

vs. CMOD curve, called compliance, is then obtained (see Figure 6 for various *a/W* ratios). The notch is then cut deeper to a value a_2 and the process is repeated. The compliance is then determined for each *a/W* ratio and a calibration curve is plotted (Figure 7). Using this calibration curve, crack growth length under 4PB can be determined by measuring the specimen compliance.

2.1.5 Subcritical crack growth (SCG) test

The fracture toughness of granite obtained by the method described in §2.1.3 is 0.766 $MPam^{1/2}$. This value is used to estimate the pre-determined load for subcritical crack growth test. Dead weight leading to 90% K_{IC} is applied to the specimen. The CMOD is recorded as a function of time throughout the duration of the test. The compliance (mm/kN) can be calculated using the applied load and the corresponding CMOD. Thus, the crack length growth (*a/W*) at the corresponding time can be determined using Figure 7. The crack growth rate *v* at each time interval can be calculated using Eq. (4).

$$v = da/dt \approx [(a_1 - a_2)/(t_1 - t_2)] \quad (4)$$

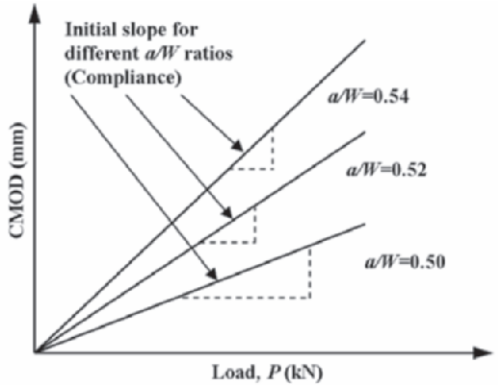

Figure 6. Determination of the initial slope of the load versus CMOD curve.

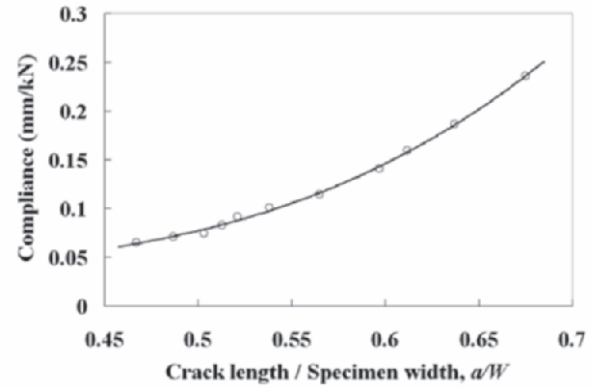

Figure 7. Compliance calibration curve of granite specimen.

where a_1 and a_2 are the crack lengths at times t_1 and t_2 respectively. The SIF, K_I is determined from the pre-determined load using Eqs.(2) and (3). Therefore, K_I/K_{IC} versus v can be plotted. To study the environmental effects, the experiments will be repeated by testing the specimens in water and in dilute sulphuric acid (H_2SO_4) and air, respectively. The experimental results of the environmental effect will be discussed in §3.1.

2.2 Double Torsion Test (DTT) method

2.2.1 Specimen preparation

The dimensions of granite specimens for the DTTs are: length 150 mm, width 60 mm and thickness 4 mm, as shown in Figure 8. Both top and bottom surfaces of the samples are grinded and polished to within a maximum tolerance of 0.05 mm of the specified size using a grinding machine according to the criteria suggested by Atkinson[9]. They were parallel within 0.025 mm.

A central axial 1 mm width groove is cut along the length of each specimen to approximately one-third of its thickness, t, using a table-cutting saw. A notch of about 10 mm long is cut in one end of each specimen along the line of axial groove. An initial crack (or so-called pre-crack) from the notch is first induced by using a displacement rate of 0.05 mm/min through a displacement control loading machine. The onset of cracking is indicated by an instantaneous slope change of the load-time curve.

2.2.2 Subcritical Crack Growth (SCG) test

SCG parameters from DTT are obtained from the load relaxation test. In this test, a pre-determined loading P_i (~90% P_c) is applied at 1.0 mm/min so that no significant crack extension occurs before relaxation. When the load P_i is reached and the crosshead is stopped, the load relaxation is recorded vs. time (Figure 9). A more detailed description of the load relaxation test is given by Henry et al.[10] and Meredith & Atkinson[11]. The SIF K_I at the crack tip is given by Williams and Evans[14] as:

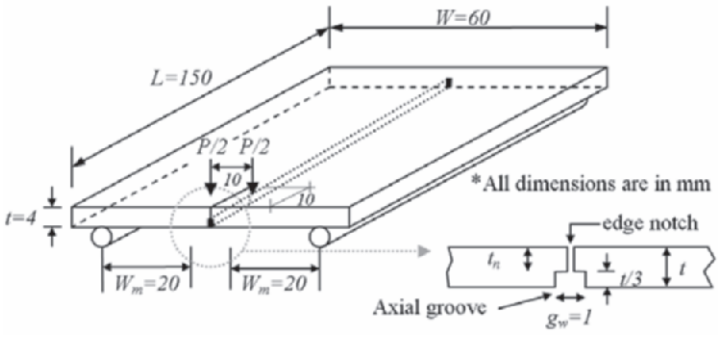

Figure 8. Schematic drawing of the double torsion specimen.

$$K_I = PW_m[3(1 + \upsilon)/Wt^3t_n]^{1/2} \quad (5)$$

where P is the corresponding load, W_m is the semi-moment arm of the specimen, υ is Poisson's ratio, W is the specimen width, t is the specimen thickness, and t_n is the reduced thickness in the plane of the groove (see Figure 8). The crack growth rate, v, is obtained as:

$$v = -(a_0P_0/P^2) \times (dP/dt) \quad (6)$$

where dP/dt is the slope of the relaxation curve at load P. The constants a_0 and P_0 are the initial crack length and the corresponding load. It is noted that the determination of both K_I and v is independent of crack length. This is regarded as one of the advantages of the double torsion test. However, it may also be viewed as a serious limitation as it is clear that stress intensity factor must depend on the crack size, no matter how small is the change.

After the relaxation test, the specimen is fractured at a rapid speed of 10 mm/min. The critical load P_C for fracturing the specimen is used to determine the fracture toughness K_{IC} from Eq.(5). The experimental results of double torsion test will be discussed in Section 3.2.

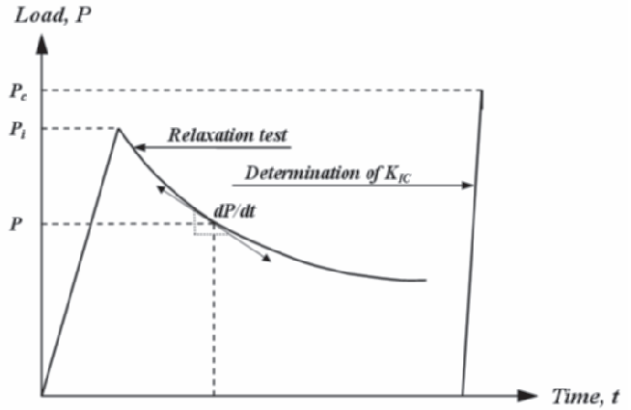

Figure 9. Schematic representation of load relaxation test. (Henry et al.[10]).

3. RESULTS AND DISCUSSION

In this section, the SCG results of both four-point bending and double torsion test are presented and compared.

3.1 Four-point bending test

The log-log plot of the crack growth rate, v, versus normalized SIF, K_I/K_{IC}, of 4PB tests on granite specimens in the environments of air, water and dilute sulphuric acid (pH value of 2) are shown in Figure 10.

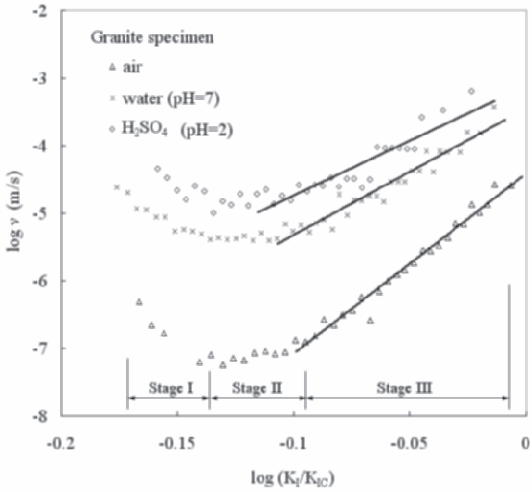

Figure 10. Log (K_I/K_{IC}) – log v curve for granite using four-point bending test.

Three stages are observed in granite specimen under different testing conditions from Figure 10. In Stage I, the crack growth rate v decreases after the application of pre-determined dead weight has been just completed. Then, v attained a minimum value when the normalized SIF (K_I/K_{IC}) reaches about 0.73, that is, log (K_I/K_{IC})= –0.137 in Figure 10. In Stage II, v becomes roughly constant over a certain range of K_I/K_{IC} while the range of K_I/K_{IC} for constant v is shorter in acidic condition (Figure 10). In Stage III, v increases and the crack propagates towards the lower edge, splitting the specimen into two pieces. To the best knowledge of the authors such a crack growth behavior with three different stages has not been reported in the literature on SCG studies using the DTT method (Figure 2). This may be due to different loading processes between 4PB test (constant loading during testing) and DTT (load relaxation during testing).

To further examine the crack growth behavior in 4PB tests, the curves of both CMODs against time are plotted (Figures 11–13), marking the three corresponding stages. It is observed that CMOD increases rapidly when applying dead weight. After weight has been applied, the CMOD increases in a smoother manner than before. The smoother displacement rate of CMOD will cause a decrease rate in crack growth velocity v in Stage I. Moreover, for testing condition in air (Figure 11b) and acid (Figures 12, 13), the difference of CMOD growth rate during and after loading becomes smaller. This is due to crack propagation during applying dead weight in both water and acidic conditions (Figures 12 and 13). Thus, the decrease level of v in Stage I is smaller in acidic condition than that in air condition. In Stage II, the CMOD grows in a nearly constant rate. However, it was found that such time for growth rate of CMOD in acidic condition is very short (Figure 13). When the crack grows to a certain length (a/W=0.56~0.59), the increase of CMOD becomes faster and such increase causes the linear increase of v in Stage III.

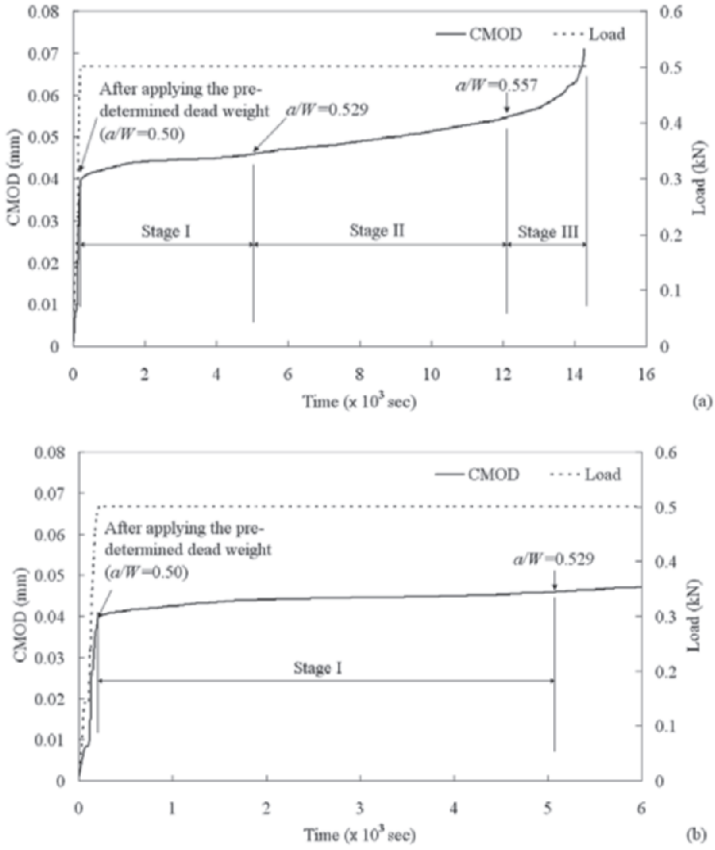

Figure 11. Curve of CMOD against time of granite specimen in air.

From Figures 11-13, it is found that the time to failure of granite specimens becomes shorter when the pH value decreases. According to Plummer et al.[17], the effects of acidic condition may be explained by the chemical weathering of feldspar mineral changing to clay mineral at the crack tip as follows:

$$H_2SO_4 \Leftrightarrow 2H^+ + SO_4^{2-} \quad \text{(Acidic condition)}$$

$$\underbrace{2KAlSi_3O_8}_{\text{Aluminosilicate minerals (feldspar)}} + H_2O + 2H^+ \rightarrow \underbrace{Al_2Si_2O_5(OH)_4}_{\text{Kaolinite (clay)}} + \underbrace{4SiO_2}_{\text{Soluble silica}} + 2K^+$$

Figure 14 shows the crack tip of the specimens after 4PB tests under microscope. By comparing the specimens it can be concluded that in air conditions (Figure14a), the minerals along the tips are weathered in a lower degree compared to those under water conditions (Figure 14b). The white colour along the crack tip is the weathered mineral (Kaolinite). On the contrary under acidic condition (Figure 14c), most of the minerals near the crack tip are weathered and changed in white colour (dotted region in Figure 14c).

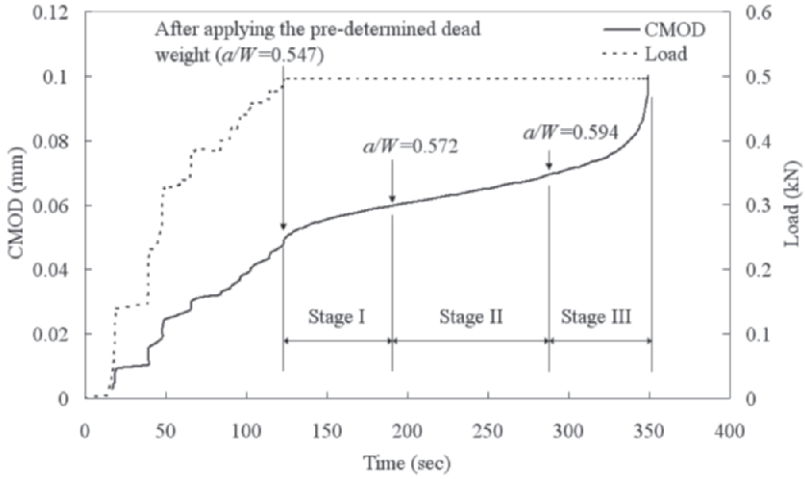

Figure 12. Curve of CMOD against time of granite specimen in water.

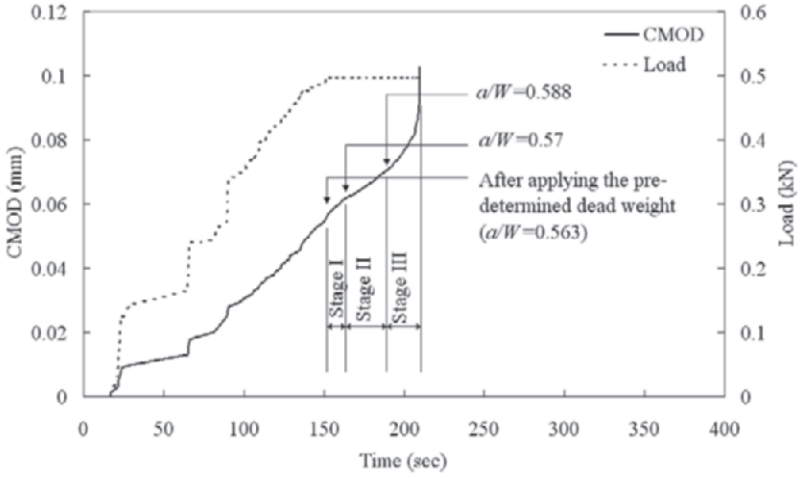

Figure 13. Curve of CMOD against time of granite specimen in H_2SO_4 (pH=2).

To determine the SCG indices *n* of granite specimens, the slope of the linear fitting in Stage III (Figure 10) is used. Table 1 compiles the *n* values of granite specimen under different environmental conditions from the 4PB test.

Table 1. The subcritical crack growth index *n* of granite using four-point bending test

Testing Conditions	Subcritical crack growth index, *n*
Air	27
Water (pH=7.0)	19
H_2SO_4 (pH=2.0)	16

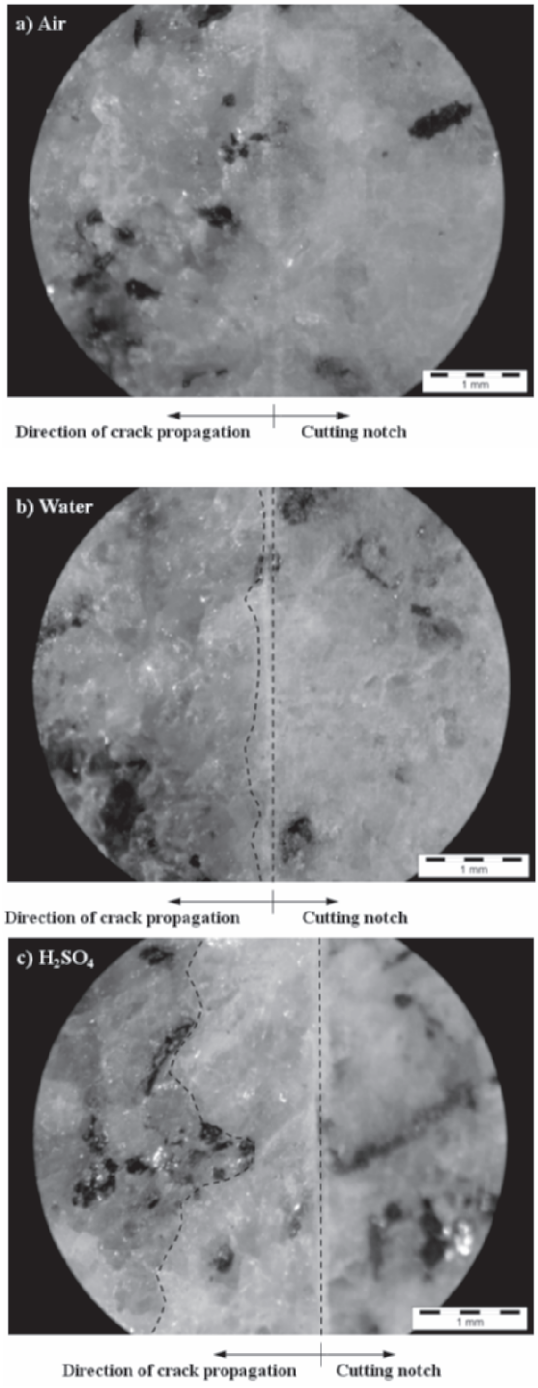

Figure 14. The crack tip of granite specimen after four-point bending test in a) air condition, b) water condition (pH=7), and c) H_2SO_4 (pH=2). Dotted region shows the weathering zone (Kaolinite) of granite specimen.

3.2 Double Torsion Test

The SCG data of load relaxation experiments on granite specimens under air, and dilute sulphuric acid (pH value of 2) is presented by a log-log plot of the crack growth rate v versus normalized K_I/K_{IC} (Figure 15).

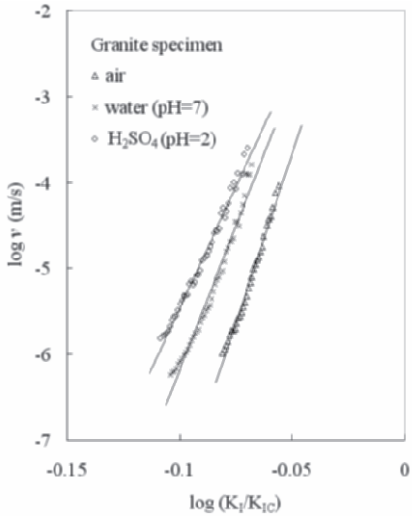

Figure 15. Log K_I – log v curve for Granite using double torsion test.

Based on the log (K_I/K_{IC}) – log v curve, it is concluded the crack growth behavior in granite rock panel (Figure 15) is similar to the behavior of Westerly granite (Figure 3) the v of which decreases during load relaxation. Furthermore, similarly to the result obtained from 4PB tests, it is found that the pH value of the aqueous environment can influence the crack growth rate at the same normalized SIF. To obtain the SCG indices n of granite specimens under different environmental conditions, the slope of the linear part of log-log plot is used (Figure 15). The SCG indices of the specimens are shown in Table 2. From this table it is concluded that the DTT data are in reasonable agreement with the upper bound of data for granitic rocks summarized by Atkinson & Meredith[18].

On the contrary, by comparing the SCG data obtained from 4PB with those from DTT, it is seen that the index n obtained from the latter is higher than that obtained from the 4PB tests by a factor of around 3.5 (Table 3). This may be due to the different fracture mechanisms activated in these test-

Table 2. The subcritical crack growth index n of granite using double torsion test

Testing Conditions	SCG index, n in this study	SCG index, n of granitic rock summarized by Atkinson & Meredith[18]
Air	92	30-90
Water pH=7.0)	69	37-68
H_2SO_4(pH=2.0)	49	Not available

Table 3. Comparison of the SCG index *n* between four-point bending and double torsion tests

Testing Conditions	SCG index, *n*		Factor (n_{DT} / n_{4PT})
	4PB test, n_{4PT}	DT test, n_{DT}	
Air	27	92	3.4
Water (pH=7.0)	19	69	3.6
H_2SO_4 (pH=2.0)	16	49	3.1

ing methods. Furthermore, as the determination of the SIF K_I from the DTT is independent of the crack length (as shown in Eq.(5)), K_I may be overestimated or underestimated for different crack lengths[19], since the crack growth length is an important parameter to determine K_I. Thus, it is worth investigating further the influence of the crack length on the results of the DTT.

4. CONCLUSIONS

Both 4PB and DTT were used to investigate subcritical crack growth of granite of rock panel under different environmental conditions. Furthermore, this is the first study to investigate SCG of granite rock panel using four-point bending test. The crack growth behavior and the SCG index *n* of both testing methods were discussed. Based on the observation and findings of this study, the following conclusions can be drawn:

- 4PB tests can be used for the study of subcritical crack growth in rock panels. The advantage of this method is that the crack growth length can be monitored by clip gauge throughout the whole test and the real situation of rock panel can be simulated.
- Three stages of K–v curve are observed in granite specimens under four-point bending test. In Stage I, the crack growth rate v decreased after the pre-determined dead weight was applied and v attained a minimum value when the normalized stress intensity factor K_I / K_{IC} reached a value of about 0.73. In Stage II, v became roughly constant over a certain range of K_I / K_{IC}. Finally, v increased and the crack propagated towards the lower edge, splitting the specimen into two pieces in Stage III.
- The crack growth behavior of granite specimens as obtained from DTT is similar to that of Westerly granite presented in previous studies.
- The pH value of the aqueous environment can influence the crack growth rate at the same normalized SIF according to the result obtained from both testing methods. Under acidic condition, crack growth rate v becomes faster than under air condition. Moreover, the time to failure of granite four-point bending specimen becomes shorter when the pH value decreases. These effects may be due to the chemical weathering of feldspar mineral changing to clay mineral at the crack tip.
- Although the SCG index *n* obtained from DTT is in reasonable agreement with the data for granitic rocks summarized in previous studies, this

value is higher than that obtained from 4PB tests, by a factor of about 3 to 4. This may be due to the different fracture mechanism activated in the two methods and the fact that the influence of the crack length on K_I is disregarded in the DTT. Thus, it is worth to investigate further the influence of crack length on the results of the DTTs.

ACKNOWLEDGEMENTS

The work described in this paper was fully supported by a grant from the Research Grants Council of the Hong Kong Special Administrative Region, China (Project No. PolyU 5166/04E). This study is part of the Master study of the first author, K.W. Kwok.

REFERENCES

1. M. Y. L. Chew, C. W. Wong and L. H. Kang, *Building Facades: A guide to common defects in tropical climates*, World Scientific Publishing Co. Pte. Ltd., pp. 12-13 (1998).
2. J. Trewhitt and J. Tuchmann, Amoco may replace marble on Chicago headquarters, *Engineering News Record* **24**, 11-12 (March 1988).
3. J. A. Bayer and C. D. Clift, Use of physical property data and testing in the design of curtain wall, *International Journal of Rock Mechanics and Mining Sciences* **30**(7), 1563-1566 (1993).
4. K. T. Chau and J. F. Shao, Subcritical crack growth of edge and center cracks in façade rock panels subject to periodic surface temperature variations, *International Journal of Solids and Structures,* **43**, 807-827 (2006).
5. B. K. Atkinson, Subcritical crack growth in geological materials, *Journal of Geophysical Research* **89**(B6), 4077-4114 (1984).
6. R. J. Charles, Static fatigue of glass, *Journal of Applied Physics* **29**, 1549-1560 (1958).
7. K. Miura, Y. Okui and H. Horii, Micromechanics-based prediction of creep failure of hard rock for long-term safety of high-level radioactive waste disposal system, *Mechanics of Materials* **35**, 587-601 (2003).
8. A. G. Evans, A simple method for evaluating slow crack growth in brittle materials, *International Journal of Fracture* **9**(3), 267-275 (1973).
9. B.K. Atkinson, Fracture Toughness of Tennessee Sandstone and Carrara Marble using the Double Torsion testing method, *International Journal of Rock Mechanics and Mining Sciences Abstracts* **16**, 49-53 (1979).
10. J. P. Henry, J. Paquet, and J. P. Tancrez, Experimental Study of Crack propagation in Calcite Rocks, *Int. J. Rock Mech. Min. Sci. & Geomech. Abstr.* **14**, 85-91 (1977).
11. P. G. Meredith, B. K. Atkinson, Fracture toughness and subcritical crack growth during high-temperature tensile deformation of Westerly granite and Black gabbro", *Physics of the Earth and Planetary Interiors* **39**, 33-51 (1985).
12. P. L. Swanson, Subcritical Crack Propagation in Westerly Granite: An Investigation into the Double Torsion Method, *Int. J. Rock Mech. Min. Sci. & Geomech. Abstr.* **18,** 445-449 (1981).
13. P. L. Swanson, Subcritical crack growth and other time- and environment-dependent behavior in crustal rocks, *Journal of Geophysical Research* **89**(B6), 4137-4152 (1984).
14. D. P. Williams and A. G. Evans, A simple method for studying slow crack growth, *Journal of Testing and Evaluation* **1**, 264-270 (1973).

15. Y. Murakami, *Stress Intensity Factor Handbook*, Vol. 1, Pergamon Press, pp. 16-17 (1987).
16. R. A. Schmidt, Fracture-toughness testing of limestone, *Experimental Mechanics* **16**(5), 161-167 (1976).
17. C. C. Plummer, D. McGeary and D. H. Carlson, Physical Geology, New York: McGraw-Hill, 9th ed., pp. 111 (2003).
18. B. K. Atkinson and P.G. Meredith, *Fracture Mechanics of Rock*, Academic Press Inc. Ltd. (London), pp. 477-525 (1987).
19. G. G. Trantina, Stress analysis of the double torsion specimen, Journal of the American Ceramic Society **60**, 338-341 (1977).